Simulation and Forecasting of Lake Erie Storm Surges[1]

DAVID J. SCHWAB

Environmental Research Laboratories, NOAA, Great Lakes Environmental Research Laboratory, Ann Arbor, MI 48104

(Manuscript received 6 April 1978, in final form 21 June 1978)

ABSTRACT

A numerical model based on the impulse response function method is used to hindcast and forecast storm surges on Lake Erie. The impulse response function method is more efficient than numerical integration of the dynamic equations when results are required at only a few grid points. Hindcasts use wind observations from seven weather stations around Lake Erie. The surge phenomenon depends on the two-dimensional structure of the wind field and on the stability of the atmospheric boundary layer over the lake. The overall correlation coefficient between computed and observed water level deviations for 15 five-day hindcast cases is 0.83 at eight water level recording stations. Operational Great Lakes wind forecasts are used to drive the model for water level forecasts at Buffalo, NY, and Toledo, OH. The accuracy of the water level forecasts is currently limited by the accuracy of the forecast winds.

1. Introduction

Based on hourly water levels recorded from 1940 to 1972, Pore *et al.* (1975) determined that the recorded Lake Erie water level at Buffalo, New York, exceeded the monthly mean level by at least 1.4 m on the average of once a year. The water level at Toledo, Ohio, dropped by at least 1.4 m with the same frequency. This abnormal departure of the water level from the mean is known as a storm surge as it is generally associated with the passage of an extratropical storm through the Great Lakes region. Storm surges are especially pronounced on Lake Erie because of its shallow depth and geographical orientation. High water caused by storm surges can cause flooding and contribute to shoreline erosion. Low water can be a hazard to navigation and may disturb hydroelectric power generation.

The purpose of this paper is to describe a method for hindcasting and forecasting storm surges on Lake Erie. This method must 1) take into account the two-dimensionality of the lake and the wind field over it; 2) resolve wind and water level changes on an hourly basis; 3) be applicable to any point on the shore of the lake; 4) incorporate the minimum dynamics required to explain observed surges; and 5) be readily applicable to operational forecasting. The method to be described is based on a hydrodynamic model of the lake. This method can be applied with the simplicity of statistical regression methods and meets all of the above constraints.

Storm surge dynamics are governed by long-wave theory, wherein the horizontal scale is much larger than the depth. By specifying wind stress on the lake surface as a time-dependent boundary condition, the mass and momentum conservation equations of long-wave theory can be integrated numerically to simulate storm surge episodes. Platzman (1963) used the dynamical method to simulate nine storm surges on Lake Erie. Wind stress over the lake was interpolated from six weather stations around the lake and taken as proportional to the square of the wind speed. The correlation coefficient between observed and computed Buffalo-minus-Toledo peak setup was 0.88. The dynamical method is useful for simulation but somewhat cumbersome for routine forecasts. Platzman (1967) designed a method for operational prediction of storm surges at Buffalo and Toledo on Lake Erie to be carried out manually at the Chicago Forecast Center. This procedure involved simplification of the dynamical theory and integration mechanics. The wind field was taken as uniform over the lake and was only allowed to change at 3 h intervals.

Platzman (1963) pointed out that the correlation between Buffalo-minus-Toledo water level setup and the square of the component of wind along the axis of Lake Erie was not much smaller than the correlation between observed and calculated setup. The implication is that a simple empirical statistical model can provide satisfactory simulation of surges. Harris and Angelo (1963) developed such an empirical model based on recorded wind and pressure at six weather stations around Lake Erie and water level data for 19 storm surge episodes. They made no assumptions about the dynamics of surges. Water

[1] GLERL Contribution No. 131.

levels were expressed as a function of the 92 wind and pressure measurements that explained the greatest amount of variance between the computed and observed water levels. Correlations of 0.87 and 0.92 were obtained for *hourly* water levels at Buffalo and Toledo, respectively, with data from dependent cases. The correlation coefficient between computed and observed *extreme* values for 11 independent cases at Buffalo was 0.96.

The statistical method was applied by Richardson and Pore (1969) to develop forecast equations at Buffalo and Toledo. Water level data for the storms considered by Harris and Angelo (1963) were used. The independent variables were taken as analyzed atmospheric pressure interpolated to 25 points corresponding to grid points of the National Meteorological Center's primitive equation model. In this way, the statistical model could be applied to operational water level forecasts by using forecast pressures in the regression equations. Correlation coefficients between observed and computed values for 11 independent cases at Buffalo and Toledo were 0.81 and 0.76, respectively. This method was subsequently adopted for operational use even though it can only be applied at points where a long record of water level data is available.

A summary of the advantages and disadvantages of statistical and dynamical methods is given by Harris (1962) who showed explicitly that the solution of the linear hydrodynamic equations for water level at a given time is simply the weighted sum of forcing terms during some period before the specified time. If the weights are thought of as regression coefficients and the forcing terms as independent variables, then the dynamical and statistical methods are equivalent. The weights or regression coefficients are analogous to a Green's function or the impulse response function for water levels. The impulse response function proves to be very useful for operational predictions. The storm surge forecast at a given point is computed as the convolution of the impulse response function for that point with the time series of observed (before forecast origin) and forecast forcing terms. The impulse response functions can be calculated from a dynamic model or determined by a statistical regression analysis, but need only be computed once. The convolution is just a summation of weighted forcing terms that can be computed manually as in Platzman (1967) or on a computer when more detailed forcing terms are used.

The storm surge models of Platzman (1963, 1967) and Harris and Angelo (1963) were not implemented operationally because they required an adequate forecast of Lake Erie winds. Feit and Barrientos (1974) developed an automated objective method to forecast winds over the Great Lakes based on the Model Output Statistics technique. Their success prompted my investigation of a storm surge model that could take advantage of the forecast wind field. It was thought that the forecast winds would provide better forcing terms than pressure forecasts because, on Lake Erie, horizontal stress on the lake surface is much larger than the force due to atmospheric pressure gradients and is more directly related to the wind field than to the pressure field.

In the present study, a linear finite-difference dynamic model was used to compute response functions for several water level recording stations on Lake Erie for lake-average forcing, interpolated two-dimensional forcing and forcing at Great Lakes wind forecast points. Fifteen storm surge simulations are summarized. The simulations improved considerably when the effect of atmospheric stability on the drag coefficient was considered. Finally, a method for calculating Lake Erie storm surges based on Great Lakes wind forecasts applicable to automated operational forecasting was developed and tested on eight cases.

2. Data

Since the present operational Great Lakes wind forecasts were instituted in 1973 and water level data for 1976 were not yet available at the time of this study, only surges in the period 1973–75 were considered. Hourly recorded water levels from the eight stations shown in Fig. 1 were obtained from the National Ocean Survey for this period. The hourly levels are expressed as instantaneous heights of water level above the 1955 International Great Lakes Datum. Water levels are recorded in hundredths of feet, but all present water level results will be reported in meters rounded to the nearest tenth. The gages have been constructed to filter out oscillations caused by surface waves. Data from Buffalo and Toledo were scanned for deviations of more than 1 m from the monthly mean. Thirty storm surge episodes were thus identified. Of these episodes, 15 were not considered because of missing water level data, missing wind data or ice cover on part of the lake. One extra episode has been included during which only a small surge was observed even though the prevailing wind conditions were indicative of a large surge. These 16 episodes were included in five-day cases starting at midnight at least 36 h before the peak surge. One case includes two episodes, leaving the 15 cases listed in Table 1 to be considered.

Wind data for the 15 cases were obtained at the seven weather stations shown in Fig. 1 from the Atmospheric Environment Service for Canadian stations and the National Climatic Center for stations in the United States. At United States stations winds are recorded as hourly values of wind speed in knots and direction to the nearest 10°. At Canadian sta-

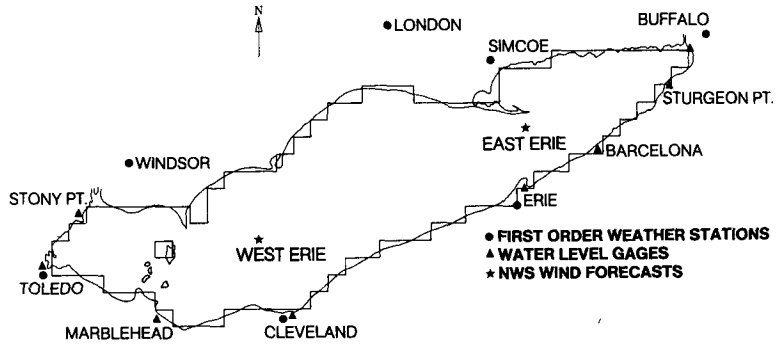

FIG. 1. Location of weather stations, water level gages and wind forecast points in relation to Lake Erie and the numerical grid.

tions speeds are recorded in miles per hour and direction in sixteen compass points. Wind speed was adjusted to a constant 6.1 m anemometer height above the ground by the power law with an exponent of 1/7.

The National Weather Service Techniques Development Laboratory supplied archived operational Lake Erie wind forecasts for eight of the cases. The wind forecasts were produced separately for the eastern and western parts of the lake at 0000 and 1200 GMT. Forecasts extend to 36 h in 6 h intervals. Wind speeds are in knots and direction in degrees.

3. Method

a. Dynamical equations

The hydrodynamic model is based on the numerical solution of the linearized, depth-integrated, shallow water equations, i.e.,

$$\left.\begin{aligned} \frac{\partial \mathbf{U}}{\partial t} &= -f\mathbf{k}\times\mathbf{U} - gD\nabla h - K\mathbf{U} + \rho^{-1}\boldsymbol{\tau}, \\ \frac{\partial h}{\partial t} &= -\nabla\cdot\mathbf{U} \end{aligned}\right\}, \quad (1)$$

TABLE 1. Dates of cases used in storm surge simulations.

Case	Dates
1	16 March–20 March 1973
2	7 April–11 April 1973
3	30 October–3 November 1973
4	4 December–8 December 1973
5	1 April–5 April 1974
6	6 April–10 April 1974
7	13 April–17 April 1974
8	27 September–1 October 1974
9	12 November–16 November 1974
10	18 November–22 November 1974
11	29 November–3 December 1974
12	10 January–14 January 1975
13	20 March–24 March 1975
14	1 April–5 April 1975
15	17 April–21 April 1975

where

- $\mathbf{U}$ transport vector
- h free surface elevation
- f Coriolis parameter
- g gravitational constant
- D water depth
- ρ water density
- K the bottom friction parameter
- $\boldsymbol{\tau}$ the wind stress vector
- ∇ the horizontal gradient
- $\mathbf{k}$ the vertical unit vector
- t time.

Forces due to atmospheric pressure gradients are neglected. The bottom stress parameter K is taken as a constant, 100 cm^2 s^{-1}, divided by the square of the water depth. This corresponds to the shallow water limit of the full Ekman layer treatment of bottom friction (see Platzman, 1963). When K is inversely proportional to the first power of the water depth, the response of the shallower parts of the lake is slightly enhanced. The boundary conditions for (1) are that τ be specified as a function of space and time and that there be no transport normal to the shoreline.

The variables in (1) are discretized on the 10 km grid shown in Fig. 1 as follows. The free surface displacement h is defined at the center of each grid box. The east-west component of $\mathbf{U}$ is defined at the midpoints of the east and west sides of the grid boxes. Similarly, the north-south component is defined at the midpoints of the north and south sides. This distribution of variables is known as a single Richardson lattice. On this grid the boundary condition of vanishing normal transport at the shoreline is directly satisfied by setting the appropriate component of $\mathbf{U}$ equal to zero. The spatial derivatives in (1) are then represented by central differences. Coriolis terms are computed as inverse depth-weighted averages. Free surface elevation h and transport $\mathbf{U}$ are calculated at alternate half time steps so that central differencing can also be

used in time. Friction terms are lagged behind Coriolis and pressure gradient terms. This Richardson lattice scheme has been used by Platzman (1972) and can be shown to be energy and mass conservative.

It was found that with the possible exception of the Coriolis terms, the above model incorporates the minimum amount of dynamics to meet the objectives outlined in the introduction. Variations in the density of the lake are neglected as are all nonlinear terms. These effects are small for free surface fluctuations of the lake. Bottom friction is simply taken as proportional to transport but this approximation provides enough damping to match the observed relaxation rate of the lake. An improvement in grid resolution would improve the model more than incorporation of density variations, nonlinear effects or a more detailed specification of the bottom friction term.

The finite-difference equations are generally solved by describing wind stress at the grid point in terms of observed or forecast winds and marching forward in time. The maximum time step in the numerical integration is limited by the condition that the fastest possible long gravity wave can travel no further than half the diagonal of a grid square in a single time step. This approach leads to a computer program that must calculate transport components and water levels at all grid points with a short time interval. Wind stress must be interpolated to all grid points with the time resolution of the numerical integration, which is usually an order of magnitude higher than the time resolution of measured or forecast winds. The direct integration approach is extremely cumbersome for operational forecasts. The impulse response function method described in the following section overcomes most of these problems.

b. Impulse response functions

For storm surge simulation and prediction, water level values are required at only a few grid points and transport components are not needed at all. Wind data for hindcasts or forecasts are only available at a few points and only at intervals that are long compared to the time step of the hydrodynamic model. The impulse response function method can take advantage of these facts in storm surge calculations.

We separately represent the components of the forcing term τ in (1) by delta function impulses and define the free surface fluctuation resulting from the x impulse as $g^x(x,y,t)$ and the response from a y impulse as $g^y(x,y,t)$. Because the system (1) is linear, the free surface solution for arbitrary uniform forcing, $\tau(t)$, is given by a convolution integral:

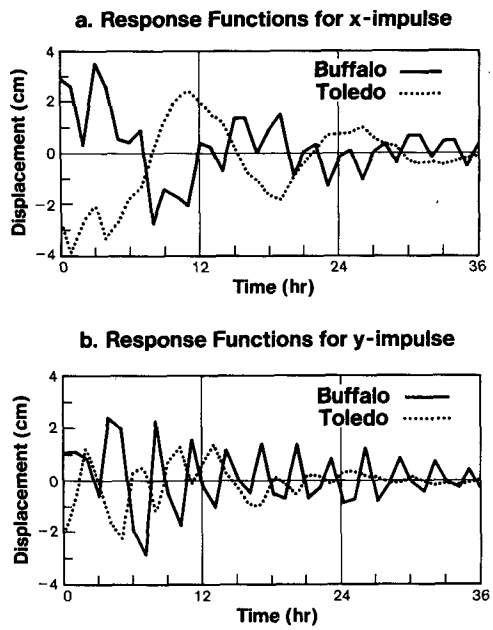

FIG. 2. Response functions for 1 dyn cm^{-2} impulsive wind stress of 1 h duration: (a) eastward impulse, (b) northward impulse.

$$h(x,y,t) = \int_{-\infty}^{t} \mathbf{g}(x, y, t - t') \cdot \tau(t') dt', \qquad (2)$$

where $\mathbf{g} = (g^x, g^y)$. The function $\mathbf{g}$ is the Green's function for water levels. In the discretized system, the impulse response functions or Green's functions are calculated by letting the individual stress components be one unit for the first time step only, integrating forward in time with no forcing and recording the $\mathbf{g}$ functions at points of interest. Then for time-dependent forcing, one need only calculate the discrete analogue of (2) to find the free surface response at any point of interest, a much simpler process than numerical integration of the finite-difference form of (1).

The forcing function τ is usually given at intervals that are long compared to the time resolution of the impulse response function, so the calculation can be further simplified by pre-summing the discrete $\mathbf{g}$ over that period. The response functions due to a spatially uniform 1 dyn cm^{-2} stress impulse for Buffalo and Toledo summed over 1 h periods are shown in Fig. 2. Calculations with time-dependent forcing use response functions that are 72 h long even though the amplitude is quite small after the first 36 h. The oscillations in the response functions correspond in frequency to the free oscillations of Lake Erie. The lowest longitudinal mode has a period of 14 h, and the lowest transverse mode a period of about 3 h. The transverse mode is more apparent after a northward impulse and the longitudinal mode after an eastward impulse.

To include spatial dependence in the wind field,

some sort of interpolation scheme must be used. It is advantageous to choose one that assigns a weighting factor w_i to the m discrete forcing terms, such as

$$\tau(x,y,t) = \sum_{i=1}^{m} w_i(x,y)\tau_i(t), \quad (3)$$

where

$$\sum_{i=1}^{m} w_i(x,y) = 1.$$

In the present model, w_i is proportional to the inverse square of the distance from station i. This interpolation formula is identical to the one used by Platzman (1963). The impulse response functions are calculated for each wind station i by letting the individual components of stress at that station be one unit for the first time step [which from (3) is equivalent to the spatial dependence of that component of τ being given by $w_i(x,y)$ for one time step], running the model for 72 h and recording the water level response. This means that for the seven wind stations used in the hindcasts, seven response functions $\mathbf{g}_i$ must be calculated for each water level station of interest. The wind-weighting functions w_i are used only for the calculation of $\mathbf{g}_i$.

By using the $\mathbf{g}_i$ calculated in this way the water level response for spatially dependent wind can be written as

$$h(x,y,t) = \sum_{i=1}^{m} \int_{-\infty}^{t} \mathbf{g}_i(x, y, t - t')\cdot\tau_i(t')dt'. \quad (4)$$

This computation is still much more efficient than a numerical integration of the finite-difference form of (1) as long as the number of surface elevation points and wind station points is considerably smaller than the total number of grid boxes.

c. Surface stress

Since wind stress τ is not measured directly, it must be specified in terms of measured or forecast winds. For hindcasts, hourly wind speed and direction at seven stations around Lake Erie are used. Air and water temperatures at one of the stations are used to provide a measure of atmospheric stability. For simulated forecasts, archived Lake Erie wind forecasts are used.

The weather station wind speed measurements S_L used in the hindcasts are converted to appropriate 10 m overlake values S_w by using the relation

$$\frac{S_w}{S_L} = \psi(S_L)\phi(T_a - T_w). \quad (5)$$

The functions ϕ and ψ are approximations to the curves developed by Resio and Vincent (1977) based on boundary layer theory and verified by Lake Erie and Lake Ontario wind speed measurements, i.e.,

$$\left.\begin{aligned} \psi &= 1.2 + \frac{1.9}{S_L(\text{m s}^{-1})} \\ \phi &= 1.0 - \left(\frac{T_a - T_w}{1900°\text{C}}\right)^{1/3} \end{aligned}\right\}, \quad (6)$$

where T_a is air temperature and T_w water temperature. These corrections are not applied to Lake Erie wind forecasts, which are based on ship observations and are already representative of overlake wind.

Vector surface stress is taken as proportional to the product of wind speed and vector wind $\mathbf{U}_i$, i.e.,

$$\rho_a^{-1}\tau_i = c_d|\mathbf{U}_i|\mathbf{U}_i. \quad (7)$$

Air density ρ_a is assumed to be a constant, 1.25 $\times 10^{-3}$ g cm^{-3}. The drag coefficient over water, c_d, is a function of wind speed and boundary layer stability. The dependence on wind speed is due to the changing roughness height z_0 caused by generation of surface waves. Charnock (1955) suggested that for a fully developed wave field the dependence can be parameterized by

$$z_0 = au_*^2/g, \quad (8)$$

where a is a constant and u_* is friction velocity (equal to the square root of the magnitude of $\rho_a^{-1}\tau$). Following the lines of Cardone (1969), a computer subroutine was developed to iteratively determine z_0, u_* and c_d over water given wind speed and air-sea temperature difference. The stability dependence of c_d is based on the Monin-Obukhov profile similarity theory presented by Businger *et al.* (1971). The constant a in (8) is chosen so that $c_d = 1.62 \times 10^{-3}$ for neutral stratification and a wind speed of 15 m s^{-1} at 10 m height as suggested by the data of Smith and Banke (1975). The numerical value of a is 0.046. The resultant dependence of c_d on wind speed and air-sea temperature difference is shown in Fig. 3. There is a rapid decrease of c_d on the stable side of the neutral curve. In unstable condi-

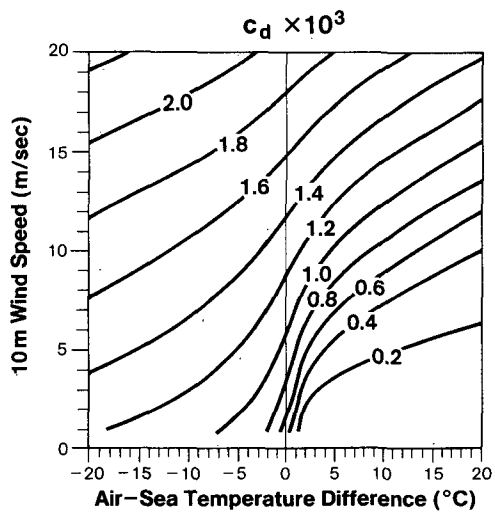

FIG. 3. Drag coefficient for 10 m wind speed.

tions and at higher wind speeds, c_d increases gradually.

Some calculations were carried out with a constant drag coefficient to compare to the variable drag coefficient results. In both cases, the actual value used for the drag coefficient was about twice the value indicated by micrometeorological measurements like those of Smith and Banke (1975). This increase in the drag coefficient is required to match observed water level fluctuation magnitudes and has always been a source of controversy. The difference between observed and computed fluctuations may be due to modification of surface slope in the region between numerical grid points and the shore. Another possible explanation is that the effective surface stress is increased because the bottom stress due to the deep return flow during a storm surge can be in the same direction as the wind. An increase in the drag coefficient may also result from the form drag on a growing wave field. In any case, the numerical values for c_d shown in Fig. 3 were multiplied by 1.8 before they were used in stress computations so that the magnitude of computed water level fluctuations would agree with observations.

4. Results

a. Hindcasts

Simulation of surges using observed hourly winds from the weather stations in Fig. 1 was done in three stages, with each successive stage incorporating a more detailed description of the forcing field. First, I ran several cases using lake-averaged wind, ignoring the dependence of overland-overlake wind differences on stability and wind speed but multiplying average wind speed by a constant factor of 1.4. I used a constant drag coefficient of 3.2×10^{-3} and employed the response functions shown in Fig. 2. Note that any combination of overland-overlake wind speed factor squared and drag coefficient with the same product as the factors used here will give identical results. Results from a typical case, 12–16 November 1974, are presented in Fig. 4a. Correlation coefficients between observed and calculated hourly water levels are calculated at each station; data from the first day of each 5-day simulation is ignored. For this case the correlation coefficient is 0.75 for Buffalo and 0.78 for Toledo. The extreme levels of the surge are modeled quite well at Toledo, but the computed peak at Buffalo on 14 November 1974 is 0.6 m compared to the observed peak of 1.9 m. However, a closer look at the wind measurements from the individual stations reveals that the maximum wind speed at Buffalo was 18 m s^{-1} at 0800 EST, while the lake average was 8.8 m s^{-1}. Several of the simulations using lake-averaged wind showed the same effect, i.e., a local wind maximum, which is not reflected in the lake-average wind but which causes a larger surge than calculations indicated. Note that the drag coefficient, which was chosen for best overall fit between computed and observed water levels, is about twice the value for 15 m s^{-1} wind speed suggested by Smith and Banke (1975).

The next step in refining the forcing field specification was to incorporate spatial variations in the wind field. Impulse response functions were computed for unit x and y impulses at all seven weather stations as outlined in the previous section. Spatially dependent stress was calculated according to (3) and (7), with a constant drag coefficient of 3.2×10^{-3} and representative overlake wind speed again taken as 1.4 times the overland measurement. Water level displacements at all eight water level recording stations were computed according to (4) for all 15 cases. The results for the 12–16 November 1974 case at Buffalo and Toledo are presented in Fig. 4b. Correlation coefficients were improved in all cases and peak water level deviations were simulated more accurately. The overall average correlation coeffi-

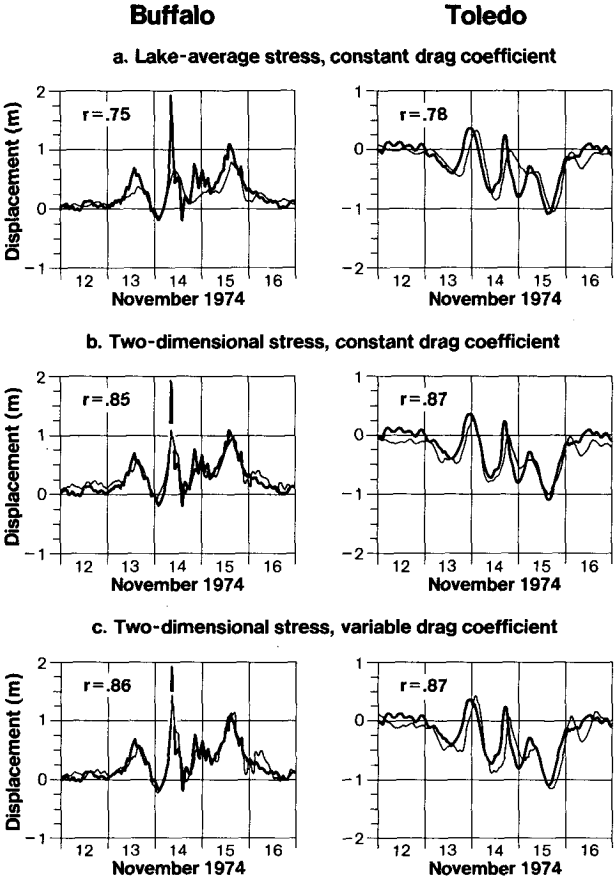

FIG. 4. Observed (heavy) and computed (light) water level deviations for 12–16 November 1974 and correlation coefficient r.

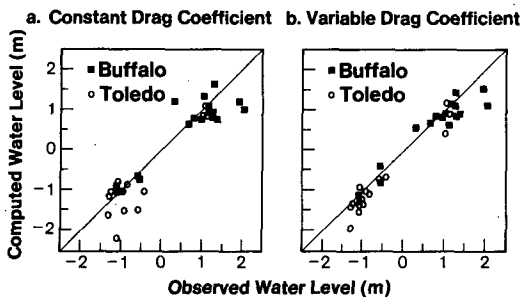

FIG. 5. Observed and computed peak water level deviations for 15 simulation cases: (a) without stability and speed dependence, (b) with stability and speed dependence.

cient for the 15 cases and eight water level stations was 0.81. Observed and computed extreme water levels are compared in Fig. 5a. Root-mean-square differences between observed and computed extremes are 0.5 m at both Buffalo and Toledo. Note that in three of the cases Toledo shows a positive surge and Buffalo a negative surge. The results of the simulations with constant drag coefficient and spatially dependent forcing are comparable to Platzman's (1963) results with a dynamic model and Harris and Angelo's (1963) statistical model.

Several cases still showed anomalously poor correlation between computed and observed water levels. Case 5, 1–5 April 1974, was included because the observed winds were high enough to cause a large surge but none was observed. This case showed the lowest correlations at nearly all stations. The following five days, 6–10 April 1974, constituted another case during which a large surge was observed and during which computed water levels agreed quite well with the observations. Computed and observed water levels during these 10 days of simulation are shown in Fig. 6. Also shown is the observed hourly difference between air and water temperature at Cleveland. By examining this case and the other cases with poor correlations, it became apparent that during periods of stable boundary layer stratification (air temperature greater than water temperature) a wind field of given strength resulted in less surface stress on the lake than during unstable periods. Since most storm surge episodes occurred during unstable conditions, the constant drag coefficient of 3.2×10^{-3} was appropriate for these cases but should have been smaller in the stable cases. As a result, the dependence of overland-overlake wind speed difference on stability and overland speed and the atmospheric boundary layer model discussed in the previous section was incorporated into the simulations to compute overlake wind speed and drag coefficient as functions of stability and wind speed. It was also necessary to increase the calculated drag coefficients by a factor of 1.8 to match observed peak water levels.

Fig. 4c shows the computational results for the 12–16 November 1974 case, with a variable drag coefficient. The difference between the computed and observed peak water level at Buffalo is reduced to 0.4 m. A summary of computed and observed

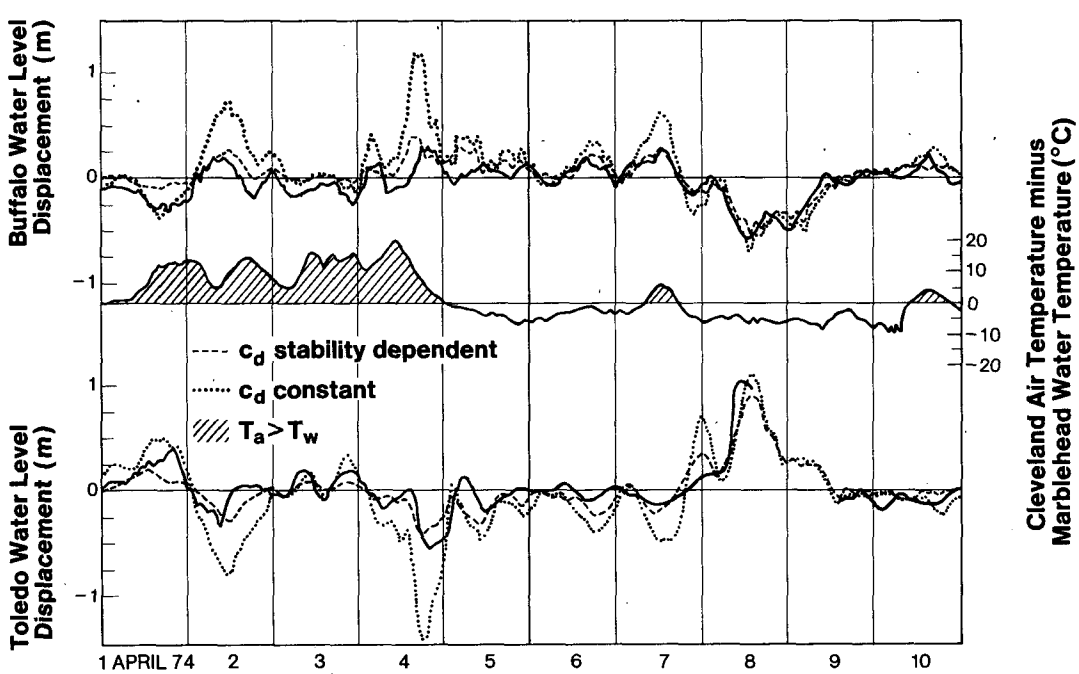

FIG. 6. Observed (solid line) and computed [(dashed line) with stability and speed dependence, (dotted line) without stability and speed dependence] water level deviations for 1–10 April 1974.

TABLE 2. Summary of computed and observed peak water level deviations and their time of occurrence for hindcast cases.

Case	Maximum displacement (m)			Time of occurrence (EST)		
	Observed	Computed	Computed minus observed	Observed	Computed	Computed minus observed (h)
			Buffalo			
1	1.0	0.9	−0.1	0000 18 March	0500	5
2	−0.6	−0.4	0.2	1700 9 April	1800	1
3	2.0	1.2	−0.8	0700 1 November	1200	5
4	1.4	1.0	−0.4	0000 6 December	0300	3
5	0.3	0.6	0.3	1800 4 April	1800	0
6	−0.5	−0.8	−0.3	1300 8 April	1300	0
7	1.3	1.5	0.2	2200 14 April	2400	2
8	0.8	0.9	0.1	1300 29 September	1500	2
9	2.0	1.6	−0.4	0800 14 November	0900	1
	1.2	1.2	0.0	1400 15 November	1500	1
10	0.7	0.7	0.0	0700 21 November	0600	−1
11	−1.1	−1.1	0.0	2000 1 December	1900	−1
12	1.2	1.2	0.0	0300 12 January	0500	2
13	1.1	0.7	−0.4	1600 22 March	1600	0
14	1.3	0.9	−0.4	0900 3 April	0900	0
15	1.0	0.9	−0.1	1100 19 April	1100	0
rms value	1.2	1.0	0.3			2.2
			Toledo			
1	−1.0	−1.3	−0.3	0400 18 March	0000	−4
2	1.0	0.5	−0.5	1600 9 April	1300	−3
3	−1.3	−1.9	−0.6	1300 1 November	1500	2
4	−1.3	−1.4	−0.1	0200 6 December	0200	0
5	−0.6	−0.7	−0.1	1900 4 April	1800	−1
6	1.1	1.2	0.1	1200 8 April	1400	2
7	−1.1	−1.5	−0.4	2300 14 April	2300	0
8	−1.0	−1.2	−0.2	1300 29 September	1500	2
9	−0.8	−1.0	−0.2	0900 14 November	0900	0
	−1.2	−1.3	−0.1	1500 15 November	1500	0
10	−1.1	−0.9	0.2	0800 21 November	1000	−2
11	1.1	1.0	−0.1	2000 1 December	1400	−6
12	−1.1	−1.3	−0.2	0500 12 January	0600	1
13	−0.4	−0.6	−0.2	1600 22 March	1600	0
14	−1.1	−1.2	−0.1	1200 3 April	1300	1
15	−0.9	−1.0	−0.1	0600 19 April	1700	11
rms value	1.0	1.2	0.3			3.5

peak water level deviations for all 15 cases is given in Table 2 and plotted in Fig. 5b. There is a tendency for the model to underestimate the peak positive surge at Buffalo and overestimate the peak negative surge at Toledo. Computed peaks generally lag observed peaks by a few hours. Overall, the rms difference between observed and computed extreme levels was 0.3 m at both Buffalo and Toledo. In case 5 (Fig. 6) the computation that includes stability dependence agrees better with observed water levels.

b. Simulated forecasts

Archived Great Lakes wind forecasts were available for eight of the 15 simulation cases. Forecasts for the two points shown in Fig. 1 are produced at 0000 and 1200 GMT for the following 36 h period in 6 h increments. It was found that the forcing field determined from the two forecast points alone was generally too high on the upwind end of the lake so Buffalo and Toledo were included as dummy forecast points. The forecasts at the Buffalo and Toledo points were the same as the eastern and western Erie forecasts, respectively, but the wind speed at the upwind station was decreased by 30%. The forcing field determined from this four-station network gave much better water level forecasts than the two forecast points alone.

Response functions for forcing at the two forecast points plus Buffalo and Toledo were computed and saved. Forecasts were then made from hourly interpolated values of forecast wind speed and direction. For the forecast simulation, no account was taken

TABLE 3. Summary of computed minus observed values of peak water level displacement and time of occurrence for 1–12, 13–24 and 25–36 h forecasts and hindcasts.

Case	Maximum displacement (m)				Time of occurrence (h)			
	25–36 h	13–24 h	1–12 h	Hindcast	25–36 h	13–24 h	1–12 h	Hindcast
				Buffalo				
3	−1.1	−0.9	−0.9	−0.8	8	3	4	5
5	0.6	1.6	1.6	0.3	−5	−6	−6	0
6	−0.1	−0.1	−0.1	−0.3	0	−2	−1	0
7	−0.1	−0.4	−0.5	0.2	11	9	9	2
8	−0.5	0.0	0.0	0.1	16	−2	−2	2
9	−1.5	−1.2	−1.3	−0.4	11	7	5	1
	−0.5	−0.4	−0.5	0.0	−11	−1	−2	1
10	0.0	0.1	0.1	0.0	−1	3	3	−1
11	0.4	0.0	0.0	0.0	−3	−1	−1	−1
rms value	0.7 m	0.8 m	0.8 m	0.3 m	8.1 h	4.2 h	4.0 h	2.0 h
				Toledo				
3	0.1	−0.1	−0.1	−0.6	2	−2	−1	2
5	−0.7	−1.9	−1.8	−0.1	5	4	4	−1
6	0.2	0.2	0.2	0.1	1	−1	0	2
7	0.1	−0.3	−0.3	−0.4	3	−4	−4	0
8	0.6	0.2	0.1	−0.2	8	−1	1	2
9	0.3	0.0	0.2	−0.2	10	6	4	0
	0.4	0.3	0.3	−0.1	−10	−1	−2	0
10	0.1	−0.1	−0.1	0.2	−1	2	2	−2
11	0.2	0.9	0.9	−0.1	−2	1	0	−6
rms value	0.4 m	0.7 m	0.7 m	0.3 m	5.8 h	3.0 h	2.6 h	2.4 h

of atmospheric stability. Forecast wind speed is already representative of overlake conditions so the drag coefficient is a constant 3.2×10^{-3}. Resultant water level forecasts at Buffalo and Toledo were split into 0–12 h, 13–24 h and 25–36 h segments. A summary of the differences between forecast and observed peak levels is presented in Table 3.

The two main sources of error in the forecasts are inadequacies in the model described in the previous section and inaccuracies in the forecast wind field. Error in the hindcast results is due mainly to model inadequacies so the difference between the hindcast and forecast errors is attributable to errors in the forecast wind field. The longer range forecasts agree better with observed peak levels, but the time of occurrence is most accurately predicted by the 1–12 h forecast. The reason the longer range forecast seems better for surge amplitude is that the long-range winds are generally underestimated and the drag coefficient used in the forecast model was chosen for best overall agreement between forecast and observed levels. Had the drag coefficient been chosen only on the basis of the 1–12 h forecasts, the longer range forecasts would severely underestimate peak levels.

Twenty-five days of sample forecasts for Buffalo and Toledo are shown in Figs. 7 and 8. The hindcasts for this period are also shown. Scales are shown in both feet and meters because operational water level forecasts are still made in feet. During this period, three large surges occurred. The 14–15 November surge is underestimated in the forecasts because the wind forecasts were poor for this storm. The 20–21 November and 1 December surges are forecast better. Both are apparent in the 25–36 h forecast, although the 1 December surge is overestimated at Toledo. The hindcast is good for the whole period so that most of the error in the water level forecast is due to error in the wind forecast.

Since Great Lakes wind forecasts are produced automatically by the National Weather Service, it is possible to use the model for automatic prediction of Lake Erie water level deviations. Maximum surges generally occur at Buffalo or Toledo but forecasts can be produced for any point on the numerical grid. The National Weather Service Techniques Development Laboratory is presently evaluating this method for possible operational implementation.

5. Conclusions

Based on the results of 15 five-day storm surge simulations and eight simulated forecasts, the following conclusions can be made:

1) Horizontal variations in the wind field over

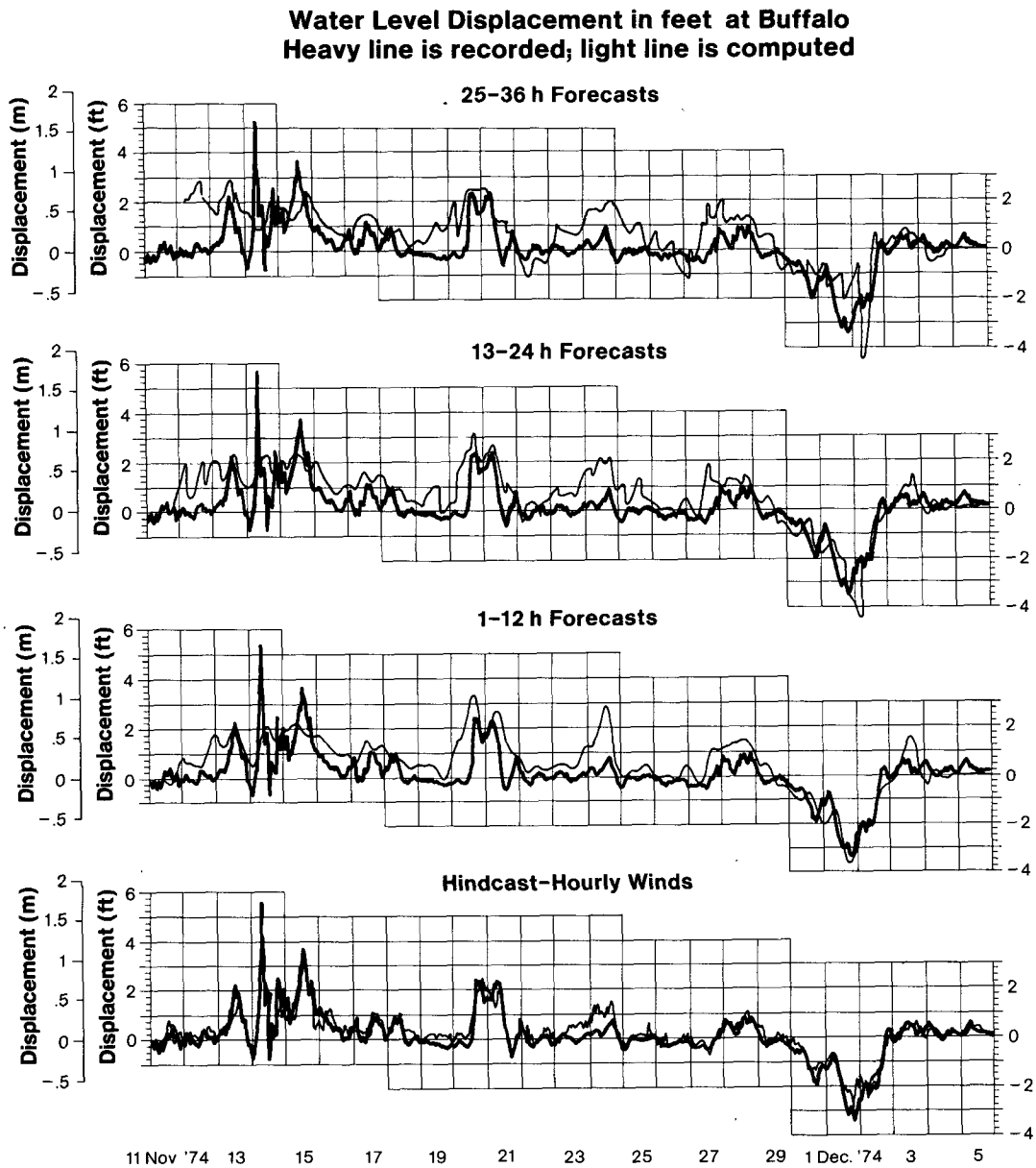

FIG. 7. Observed water level deviations (heavy), and forecasts and hindcasts (light) for Buffalo.

the lake can be as important as the mean wind field in determining surges. Peak water level deviations are sensitive to the local as well as to the lake average wind.

2) Atmospheric boundary layer stability significantly affects momentum transfer to the lake. To simulate storm surge phenomena under a variety of stability regimes, the drag coefficient in the standard parameterization of surface stress must be a function of the air-sea temperature difference. The dependence of the drag coefficient on wind speed is less significant, but when it is included it does improve verification of peak water levels.

3) Drag coefficients used in this study are about twice as large as those indicated by wind profile and eddy correlation measurements in the marine boundary layer. This is consistent with previous storm surge simulation studies. Some reasons for this discrepancy are nearshore effects, inaccurate parameterization of bottom stress and the effect of surface waves on momentum transfer during high wind conditions. As with most storm surge studies, the results reported here are biased toward storm conditions. The peak water level deviations at Buffalo and Toledo (Fig. 5) suggest that computed water levels are too low on the downwind end of the lake and too high on the upwind end. The effect of surface waves may explain this discrepancy.

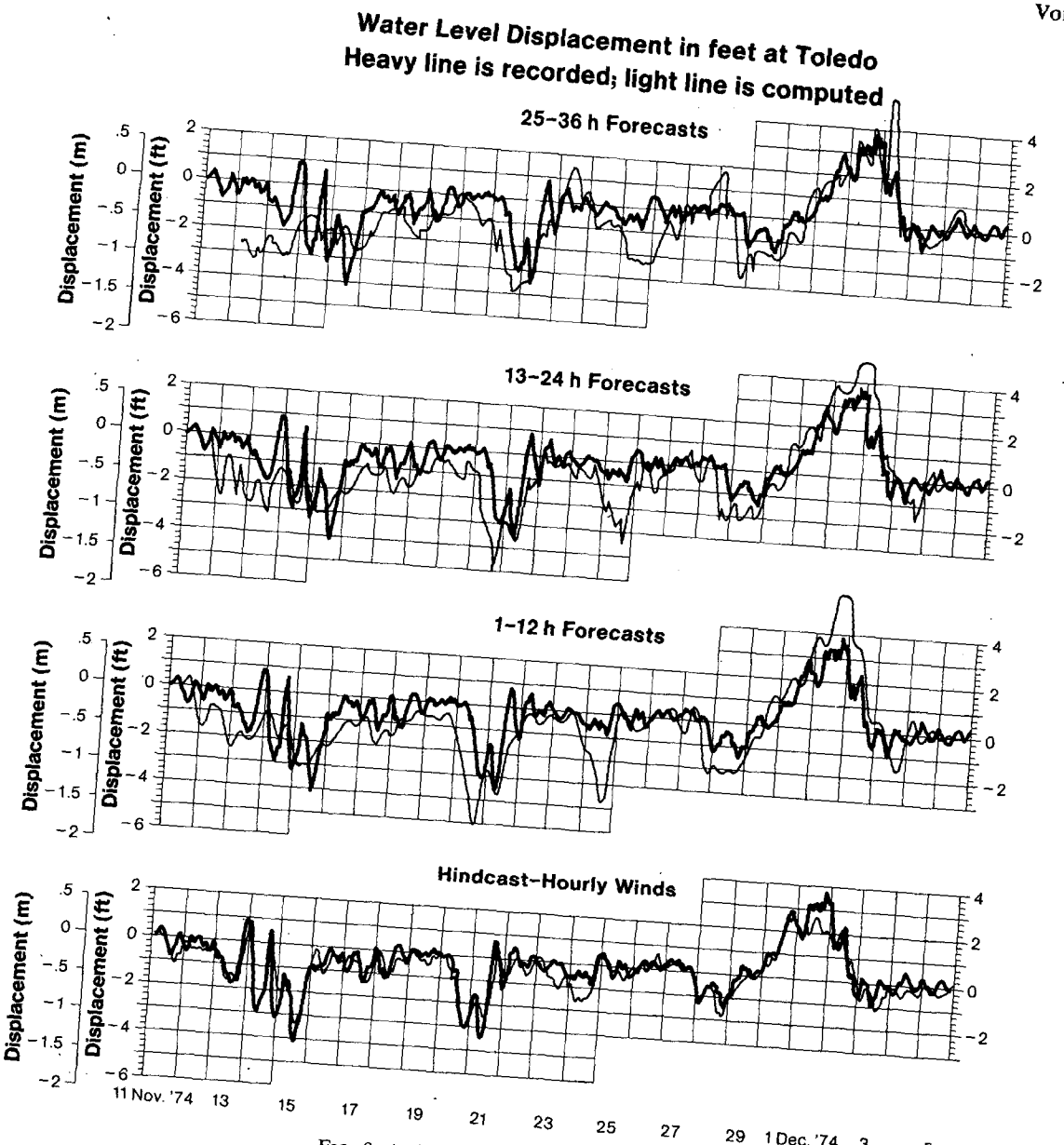

FIG. 8. As in Fig. 7 except for Toledo.

4) The results of storm surge hindcasts show that the model is capable of accurately predicting Lake Erie water level deviations from wind observations taken at seven stations around the lake. For 15 hindcast cases, the rms difference between computed and observed maximum deviations at Buffalo and Toledo is 0.3 m. Predictions based on Great Lakes wind forecasts at two points in Lake Erie are not as accurate as the hindcasts but may still be useful as forecast tools. The main source of error in water level forecasts is the meteorological forecast; that error is larger than errors due to inadequacies of the model.

Acknowledgments. I would like to thank Richard Nelis of the Atmospheric Environment Service for his assistance in obtaining the Canadian wind data and Daniel Mitchell of the National Climatic Center for providing wind data for the U.S. stations. William Richardson and David Feit of the National Weather Service Techniques Development Laboratory were extremely helpful in developing the operational forecasting procedure. John Bennett and Janice Boyd formulated the computer subroutine for the drag coefficient.

REFERENCES

Businger, J. A., J. C. Wyngaard, Y. Izumi and E. F. Bradley, 1971: Flux-profile measurements in the atmospheric surface layer. *J. Atmos. Sci.*, **28**, 181–189.

Cardone, V. J., 1969: Specification of the wind distribution in the marine boundary layer for wave forecasting. Rep. TR-69-1, Contract Nonr 285(57), Dept. Meteor. Oceanogr., New York University, 131 pp. [NTIS AD-702490].

Charnock, H., 1955: Wind stress on a water surface. *Quart. J. Roy. Meteor. Soc.*, **81**, 639.

Feit, D. M., and C. S. Barrientos, 1974: Great Lakes wind forecasts based on model output statistics. *Proc. 17th Conf. Great Lakes Res.*, 725–732 Int. Assoc. Great Lakes Res., Ann Arbor. [University Microfilms].

Harris, D. L., 1962: The equivalence between certain statistical prediction methods and linearized dynamical methods. *Mon. Wea. Rev.*, **90**, 331–340.

——, and A. Angelo, 1963: A regression model for storm surge prediction. *Mon. Wea. Rev.*, **91**, 710–726.

Platzman, G. W., 1963: The dynamical prediction of wind tides on Lake Erie. *Meteor. Monogr.*, No. 26, 44 pp.

——, 1967: A procedure for operational prediction of wind set-up on Lake Erie. Tech. Rep. No. 11, Contract 91-67(N), Dept. Geophys. Sci., The University of Chicago, 93 pp. [NTIS PB-178336].

——, 1972: Two-dimensional free oscillations in natural basins. *J. Phys. Oceanogr.*, 2, 117–138.

Pore, N. A., H. P. Perrotti and W. S. Richardson, 1975: Climatology of Lake Erie storm surges. NOAA Tech. Memo. NWS TDL-54, 27 pp. [NTIS COM-75-10587].

Resio, D. T., and C. L. Vincent, 1977:Estimation of winds over the Great Lakes. *J. Waterway Port Coast. Ocean Div., ASCE*, **102**, 265–283.

Richardson, W. S., and N. A. Pore, 1969: A Lake Erie storm surge forecasting technique. ESSA Tech. Memo. WBTM TDL 24, 23 pp. [NTIS PB-187778].

Smith, S. D., and E. G. Banke, 1975: Variation of the sea surface drag coefficient with wind speed. *Quart. J. Roy. Meteor. Soc.*, **101**, 665–673.